Synthesis and Structure of $Ca_{14}GaP_{11}$ with the New Hypervalent P_3^{7-} Anion. Matrix Effects within the Family of Isostructural Alkaline-Earth Metal Pnictides[1]

J. T. Vaughey and John D. Corbett*

Ames Laboratory—DOE and Department of Chemistry, Iowa State University, Ames, Iowa 50011

Received August 21, 1995. Revised Manuscript Received December 19, 1995[⊗]

The new Zintl phase $Ca_{14}GaP_{11}$ has been synthesized and studied by single-crystal X-ray diffraction. The compound is isostructural with $Ca_{14}AlSb_{11}$ and contains as separate anions a GaP_4^{9-} tetrahedron, the novel hypervalent linear P_3^{7-}, and four isolated P^{3-}. The phase is tetragonal, space group $I4_1/acd$ (No. 142) with $Z = 8$, $a = 15.347$ (4), $c = 20.762$ (8) Å (296 K), $R(F)/R_w = 3.6/5.0\%$ for 759 reflection ($I/\sigma(I) > 3$) and 63 variables. The central P4 atom in P_3^{7-} refines with its position split by 0.82 Å which in the limit corresponds to disordered P^{3-} and P_2^{4-}. Matrix effects in all 20 refined pnictide (Pn = P−Bi) examples of this structure are reflected by the cation environment about the Pn_7^{3-} anions. This approach provides complete correlation of the splittings of the central Pn4 atoms (or their displacement ellipsoid asymmetry) and the average distances in Pn_7^{3-}. Increased asymmetry of and bond lengths in Pn_3^{7-} and, by implication, lesser phase stability are logically associated with smaller Pn, larger cations, and, to a smaller degree, increased size of the metal that centers the MPn_4 tetrahedra. Angular distortions of the last are similarly based.

Introduction

Recent synthetic efforts by a number of groups have established that the family of tetragonal Zintl compounds $Ae_{14}MPn_{11}$ (Ae = alkaline-earth metal or Eu, Pn = pnictogen (As−Bi), M = Mn, Zn, Cd, Nb, or one of the triel elements Al−In) is an extensive one that is evidently rather flexible as far as ion sizes and, to some extent, composition. The structural prototype of this family, $Ca_{14}AlSb_{11}$, was first reported by Cordier et al. in 1984, with the composition and structure determined by single crystal X-ray diffraction methods.[2] Its constitution of 14 Ca^{2+}, $AlSb_4^{9-}$, Sb_3^{7-}, and 4 Sb^{3-} ions is especially significant in its diversity and in the formation of the unusual linear Sb_3^{7-} anion. More recent efforts by Kauzlarich and co-workers[3−6] have extended this structural family considerably to include several other combinations within the above groups of elements. In addition, they found that the triel atom could be replaced by manganese to yield unusual ferromagnetic compounds containing high spin d^4 Mn(III).[7−9] Notably, one of the major contributions of this group throughout has been the confirmation of the semiconducting nature of many of these phases, the expectation for a Zintl phase, and an affirmation of the oxidation state distribution proposed for these systems.[10] Incorporation of zinc or cadmium into the M site in place of the trivalent element, plus additional Pn elsewhere, has also been reported,[11] while another group has established and studied the nominally isostructural members $Ae_{13}NbAs_{11}$, Ae = Sr, Eu, which have fractional cation vacancies.[12] A theoretical study has also afforded good support for a hypervalent (3-center−4-electron) bonding scheme in the Pn_3^{7-} anions that is required by the overall compositions, ions that are isoelectronic with I_3^- and the like.[13] In this paper, we report the first phosphide example of this structural type, $Ca_{14}GaP_{11}$, along with a discussion of its relationship to other members of this family. Some generalities are developed in terms of cation matrix effects to correlate the centric versus acentric (disordered) and elongated examples of the Pn_3^{7-} anions among all members of this structure type.

Experimental Section

Sample Preparation. The general techniques were as previously described.[14] All materials were handled in a N_2-filled glovebox that had a moisture level below 0.1 ppm (vol.). The initial crystals of the title phase were isolated from the

⊗ Abstract published in *Advance ACS Abstracts,* February 1, 1996.
(1) This research was supported by the Office of Basic Energy Sciences, Materials Science Division, U.S. Department of Energy. The Ames Laboratory is operated for the DOE by Iowa State University under Contract No. W-7405-Eng-82.
(2) Cordier, G.; Schäfer, H.; Stelter, M. *Z. Anorg. Allg. Chem.* **1984**, *519*, 183.
(3) Kauzlarich, S. M.; Kuromoto, T. Y.; Olmstead, M. M. *J. Am. Chem. Soc.* **1989**, *111*, 8041.
(4) Kauzlarich, S. M.; Thomas, M. M.; Odink, D. A.; Olmstead, M. M. *J. Am. Chem. Soc.* **1991**, *113*, 7205.
(5) Kauzlarich, S. M.; Kuromoto, T. Y. *Croat. Chem. Acta* **1991**, *64*, 343.
(6) Brock, S. L.; Weston, L. J.; Olmstead, M. M.; Kauzlarich, S. M. *J. Solid State Chem.* **1993**, *107*, 513.
(7) Kuromoto, T. Y.; Kauzlarich, S. M.; Webb, D. J. *Chem. Mater.* **1992**, *4*, 435.
(8) Rehr, A.; Kuromoto, T. Y.; DelCastillo, J.; Webb, D. J.; Kauzlarich, S. M. *Chem. Mater.* **1994**, *6*, 93.
(9) Rehr, A.; Kauzlarich, S. M.; Kuromoto, T. Y. *J. Alloys Compd.* **1994**, *207/208*, 424.
(10) (a) Zintl, E.; *Angew. Chem.* **1939**, *52*, 1. (b) Schäfer, H. *Annu. Rev. Mater. Sci.* **1985**, *15*, 1. (c) Nesper R. *Angew. Chem., Int. Ed. Engl.* **1991**, *30*, 789.
(11) Young, D. M.; Torardi, C. C.; Olmstead, M. M.; Kauzlarich, S. M. *Chem. Mater.* **1995**, *7*, 95.
(12) Vidyasagar, K.; Hönle, W.; von Schnering, H.-G. *Z. Kristallogr. Suppl. 5* **1992**, 254.
(13) Gallup, R. F.; Fong, C. Y.; Kauzlarich, S. M.; *Inorg. Chem.* **1992**, *31*, 115.
(14) Zhao, J.-T.; Corbett, J. D. *Inorg. Chem.* **1995**, *34*, 378.

0897-4756/96/2808-0671$12.00/0

Table 1. Single-Crystal Refinement Information for $Ca_{14}GaP_{11}$

empirical formula	$Ca_{14}GaP_{11}$
formula wt	971.6
crystal dimens, mm	0.4 × 0.1 × 0.1
lattice parameters (Å, Å^3)[a]	
a	15.347(4)
c	20.762(8)
V	4890(1)
space group, *Z*	$I4_1/acd$ (No. 142), 8
d_{calc} (g/cm^3)	2.641
temp (°C)	23
octants collected, 2θ limit	$h,k,\pm l$, 50°
absorption coeff (cm^{-1}, Mo Kα)	47.06
transm coeff range	0.9096−1.00
residuals, R/R_w,[b] %	3.60/5.00

[a] Lattice parameters are from least-squares refinement of Guinier powder pattern data, $\lambda = 1.540\ 562$ Å. [b] $R = \sum||F_o| - F_c||/|F_c|$; $R_w = \sum||F_o| - |F_c||w^{1/2}/\sum|F_o w^{1/2}|$; $w = 1/\sigma^2$.

composition "Ca_3Ga_4P" prepared by weighing stoichiometric amounts of the elements calcium (APL Engineering Materials, 99.99%), phosphorus (Aldrich, 99.999%), and gallium (Johnson-Mathey, 99.99%) into a tantalum tube on which one end had been previously welded. The tantalum tube was then crimped and welded shut. This reaction vessel was then placed inside a silica jacket that was evacuated and sealed. The mixture was then heated slowly to 1000 °C, held for 3 days, and then slowly cooled to room temperature over a 1-week period. There was no evidence of attack of the container. A single-phase sample of the compound (to X-rays) was subsequently synthesized by mixing stoichiometric amounts of the component elements and repeating the above procedure.

The initial product had a silvery appearance and was brittle. Several crystals from this sample were sealed into thin-walled capillary tubes. Analysis of the sample by Guinier X-ray powder diffraction, with the aid of NIST silicon as an internal standard, showed that the products of the first reaction were a mixture of hitherto unknown $Ca_{14}GaP_{11}$ and $CaGa_2$ ($CaIn_2$-type).[15] The tetragonal lattice constants of the former refined with the aid of 27 lines from the powder pattern and a nonlinear least-squares method are $a = 15.347(4)$ Å and $c = 20.762(8)$ Å.

Laue photographs were used to determine which crystal was most suitable for structural determination. Diffraction data were collected from one crystal at room temperature on a Rigaku AFC6R diffractometer with the aid of Mo Kα radiation. Cell constants and an orientation matrix for data collection were determined from a least-squares refinement of the setting angles of 25 centered reflections. In total, 4691 reflections were measured for the primitive cell in the $h,k,\pm l$ octants up to $2\theta = 50°$, and 2752 reflections among these had $I > 0$. With an absorption correction based on three psi scans, the data reduced to 1293 independent observations ($R_{ave} = 9.4\%$, $I \geq 0$) of which 759 were observed ($I/\sigma(I) > 3$). Systematic absences in the data set uniquely indicated the space group $I4_1/acd$ (No. 142), in agreement with that reported for the $Ca_{14}AlSb_{11}$ structure type and its other analogues.[2] The structure was solved by direct methods with the aid of the program package TEXSAN.[16] The anisotropic refinement of all atoms resulted in R, R_w values of 3.6, 5.0% at convergence. The maximum and minimum peaks in the final difference Fourier map were 0.70 e/Å^3 (1.1 Å from Ga1) and −1.06 e/Å^3.

The powder pattern calculated for this structure agreed very well with that observed for the pure sample synthesized. Some crystal and refinement data are given in Table 1, the atom positions and isotropic-equivalent ellipsoid values are listed in Table 2, and the anisotropic temperature factors appear in Table 3. Additional crystallographic and refinement data are given in the supporting information. These as well as the F_o/F_c data are also available from J.D.C.

Table 2. Atomic Positions and Isotropic Equivalent Thermal Parameters for $Ca_{14}GaP_{11}$[a]

atom	*x*	y	z	B_{eq} (Å^2)
Ga1	0	$^1/_4$	$^3/_8$	1.32(4)
Ca1	−0.0412(1)	−0.0723(1)	0.82843(8)	0.94(7)
Ca2	−0.0269(1)	0.1188(1)	0.00657(9)	1.19(7)
Ca3	0.3501(1)	0	$^1/_4$	0.78(9)
Ca4	0.1777(1)	0.4071(1)	0.84315(8)	1.10(7)
P1	0.1350(1)	$^1/_4 + x$	$^1/_8$	0.89(6)
P2	0.0057(1)	0.1124(1)	0.8070(1)	1.19(9)
P3	0.8712(1)	0.9719(1)	0.9530(1)	0.88(8)
P4[b]	−0.0189(3)	$^1/_4 + x$	$^1/_8$	2.5(2)

[a] Space group $I4_1/acd$, origin at the inversion center. [b] The P4 position is 50% occupied as it is split by the perpendicular 2-fold axes through $(0,^1/_4,^1/_8)$, symmetry 222.

Results and Discussion

A view of one-half of the unit-cell contents for $Ca_{14}GaP_{11}$ is shown in Figure 1. This compound contains three separate anionic components: a GaP_4^{9-} tetrahedron ($\bar{4}$ symmetry), a linear and ideally centric P_3^{7-} anion (222 symmetry) isoelectronic with the triiodide anion I_3^-, and four isolated P^{3-} anions. The sum of the charges (oxidation states) on these anions is counterbalanced by 14 Ca^{2+} cations, and the compound should be a semiconductor according to Zintl's concepts.[10,17] The tetrahedra and the trimers alternate along the $\vec{b}$ and $\vec{c}$ directions, with both ions rotated 90° each time relative to their previous orientations, as readily seen in Figure 1 along the vertical 2-fold axis that lies parallel to the *c* axis. The isolated phosphide anions are located between the columns formed by the complex anions. Selected bond distances and angles are given in Table 4.

The GaP_4^{9-} (4b-Ga^-, 1b-P^{2-}) tetrahedra are fairly routine components of the structure. They are slightly compressed along the 2-fold axis (112.59(9)° vs 107.93(5)°) compared with the ideal. This compression is commonly observed in this structural family, and its variation has been attributed to the packing constraints, cation size, and general interionic interactions. The Ga−P distance within the tetrahedron, 2.540(2) Å, is somewhat long in comparison with the Ga−P distance of 2.35 Å in the three dimensional structure of GaP.[18] Such differences among M−Pn bond lengths in this family of compounds have been attributed to a lack of shared vertexes and the high formal charge on each pnictide in the tetrahedron.[6]

As in many examples of this structure type, the central atom of the unusual P_3^{7-} trimer in $Ca_{14}GaP_{11}$ refines distinctly better off of the central 222 position and split into two 50% sites with an apparent separation of 0.82(1) Å. The shorter P4−P1 distance in the trimer is 2.520(7) Å, and the longer is 3.34 Å. On the other hand, if the P4 position is not split, so that the two distances are both 2.93 Å, the isotropic temperature factor then rises from 2.5(2) to 10.3(4) e/Å^2 and the anisotropic displacement parameters develop an extreme asymmetry (9.2:1 in the *a*−*b* plane). The phosphorus−phosphorus single-bond distances in the Zintl phases CaP_3 and Rb_2P_3 span 2.15 to 2.25 Å,[19,20] while the normal-valent triphosphide P_3^{5-} in LaP_2 also has

(15) Iandelli, A. Z. *Anorg. Allg. Chem.* **1964**, *330*, 221.
(16) TEXSAN, version 6.0, Molecular Structure Corp., The Woodlands, TX, 1990.
(17) Hughbanks, T. In *Inorganometallic Chemistry;* Fehlner, T., Ed.; Plenum Press: New York, 1992; p 291.
(18) Mohanal, S. K.; Padiyan, D. P. *Z. Kristollogr.* **1986**, *177*, 177.
(19) Schmettow, W.; Lipka, A.; von Schnering, H.-G. *Angew. Chem.* **1974**, *86*, 379.

Table 3. Anisotropic Thermal Factors for $Ca_{14}GaP_{11}$[a]

atom	U_{11}	U_{22}	U_{33}	U_{12}	U_{13}	U_{23}
Ga1	0.0176(6)	0.0176	0.015(1)	0	0	0
Ca1	0.0107(8)	0.0145(8)	0.0106(9)	−0.0015(6)	0.0018(6)	−0.0009(6)
Ca2	0.0117(8)	0.0158(9)	0.018(1)	0.0067(6)	0.0000(6)	0.0047(7)
Ca3	0.010(1)	0.010(1)	0.010(1)	0	0	0.0009(8)
Ca4	0.0095(8)	0.022(1)	0.0102(9)	0.0005(6)	−0.0015(6)	−0.0041(6)
P1	0.0125(9)	0.0125	0.009(1)	0.004(1)	0.0004(8)	−0.0004
P2	0.010(1)	0.021(1)	0.015(1)	−0.0052(8)	0.0001(8)	0.0040(9)
P3	0.016(1)	0.010(1)	0.007(1)	0.0014(7)	0.0005(8)	0.0002(7)
P4	0.033(3)	0.033	0.030(4)	−0.005(3)	0.001(3)	−0.001

[a] $U_{ij} = \exp[-2\pi^2(U_{11}h^2a^{*2} + U_{22}k^2b^{*2} + U_{33}l^2c^{*2} + U_{12}hka^*b^* + U_{13}hla^*c^* + U_{23}klb^*c^*)]$.

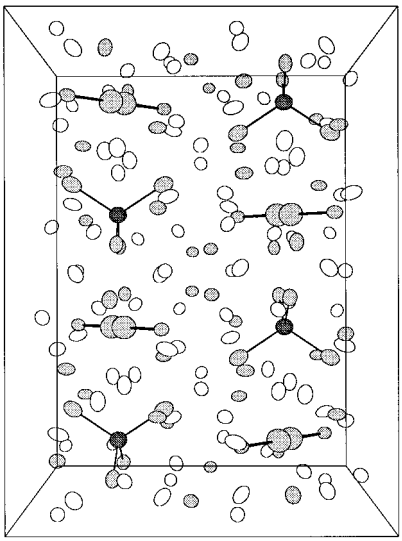

Figure 1. [100] view of the contents of one-half of the unit cell of $Ca_{14}GaP_{11}$. Calcium has open ellipsoids while phosphorus and gallium are shaded. Both of the disordered (50%) central positions in the linear P_3^{7-} are shown (99% displacement ellipsoids). The GaP_4^{9-} and P_3^{7-} anions lie on a vertical 2-fold axis parallel to $\vec{c}$.

Table 4. Selected Bond Distances (Å) and Angles (deg) for $Ca_{14}GaP_{11}$

Ga1−P2 ×4	2.541(2)	P3−Ca1	2.992(3)
Ca2 ×4	3.419(2)		2.946(3)
		Ca2	2.960(3)
P1−P4	2.520(7)		2.890(3)
Ca1 ×2	2.947(2)	Ca3 ×2	2.878(3)
Ca2 ×2	2.967(2)	Ca4	3.019(3)
Ca3 ×2	3.147(1)		3.035(3)
Ca4 ×2	2.969(3)		
P2−Ca1	2.958(3)	P4−P1	2.520(7)
	2.968(3)		3.340(7)
Ca2	2.887(3)	Ca1 ×2	2.780(3)
Ca3 ×2	3.046(3)		3.188(4)
Ca4	2.928(3)	Ca2 ×2	3.005(3)
	3.175(3)		
Ca1−Ca1	3.538(3)	Ca2−Ca2	4.111(3)
	3.940(3)		3.749(3)
Ca2	3.741(2)	Ca3	3.438(2)
	3.819(2)	Ca4	3.978(2)
	3.652(3)		3.574(2)
Ca3	3.533(2)		4.126(3)
Ca4	3.302(2)		
	4.104(2)	Ca3−Ca4 ×2	3.442(2)
	4.144(2)		3.574(2)
		Ca4−Ca4	3.821(3)
P2−Ga1−P2	107.97(5)		
	112.51(9)		

P−P distances in the normal range, 2.20 and 2.23 Å, with a bond angle of 107.62°.[21] The elongated bonds in the symmetric Pn_3^{7-} units have generally been described in terms of a hypervalent three-center− four-electron bonding scheme, isoelectronic with I_3^- and with a bond order of 0.5 per atom pair. An ab initio SCF treatment of solid $Ca_{14}GaAs_{11}$ has shown this to be an accurate assessment of As_3^{7-} in the condensed state as well.[13] The distortions implied by the disordered (off-center) Pn4 atoms that are often found in the center of other Pn_3^{7-} trimers are reminiscent of, but unrelated to, the static asymmetries found for I_3^- in the presence of smaller and higher field cations.

All of the Pn_3^{7-} distortions found in the family of novel $Ae_{14}MPn_{11}$ phases can be consistently accounted for in terms of a matrix effect generated within and by the particular surrounding cations, together with a second-order role of the nearest-neighbor MPn_4^{9-} anions. By matrix effects[22] we mean distance and other structural parameters of, here, the pnictogen components that are determined largely by closed shell/Coulombic repulsions between, in these cases, the Ae cations. The large variety of phases achieved with this structure (Ae = Ca−Ba, Eu; M = Ga, Al, Mn, Nb, Zn, Cd; Pn = P−Bi), about 25 in all, is good evidence of the stability not only of this particular structure but of each of its anionic components as well. Both band theory and resistivities (10^3−10^5 $\mu\Omega$/cm at room temperature[3−9]) indicate that the electronic states of these anions must be fairly well localized. The Pn_3^{7-} anions have relatively high charge densities, although these are rather spread out in comparison with those of the MPn_4^{9-} anions. A closer examination of the surrounding Ae^{2+} cations, especially as to their relative sizes and large number, shows that the distortions of Pn_3^{7-} should and must arise in many examples of this given structure type. The situation for the P_3^{7-} example, with the largest splitting so far reported, is shown in Figure 2 to guide the discussion.

To make the interpretations clear, Table 5 contains data reported for all compounds with this structure that have been refined from X-ray single-crystal data. These are ordered by (1) Pn size, (2) Ae (+Eu) size, and (3) within these, by the size of the MPn_4 anions. The order for the last is fairly easy to estimate for series with fixed Ae and Pn from the *a* lattice dimensions (see Figure 1); Ga∼Al < Mn (∼Nb) < Zn < Cd. With the components so arranged, Table 5 also lists (a) the refined splitting of the Pn4 site, if any (a value that may not be terribly accurate in some cases because of the proximity of the two components), (b) the appropriate $(U_{11} + U_{12})/(U_{11} - U_{12})$ measure[23] of the asymmetry of the Pn4 ellipsoid normal to $\vec{c}$ when this position was not split in the refinement ($U_{11} = U_{22}$, $U_{13} = U_{23} = 0$), and (c) the

(20) Dahlmann, W.; von Schnering, H.-G. *Naturwissenschaften* **1973**, *60*, 518.
(21) von Schnering, H.-G.; Wichelhaus, W.; Schulze-Nahrup, M. *Z. Anorg. Allg. Chem.* **1975**, *412*, 193.
(22) Corbett, J. D. *J. Solid State Chem.* **1981**, *37*, 335.

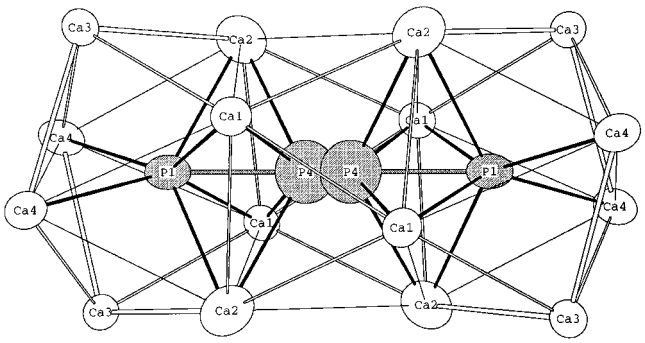

Figure 2. Illustration of the P_7^{3-} anion and its cation environment refined for $Ca_{14}GaP_{11}$, with both of the 50% P4 positions drawn. The P−Ca distances marked with solid lines range between 2.78 (P4−Ca1) and 3.00 Å. The Ca−Ca separations are: wide double lines, 3.44 Å; narrow double lines, 3.53−3.74 Å; single lines, 3.82−4.11 Å (99%).

Table 5. $Ae_{14}MPn_{11}$ Phases: Regularities in Parameters for the Central Pn4 in Pn_3^{7-} and the Angles in MPn_4^{9-}[a]

Pn	$Ae_{14}MPn_{11}$	split (Å) of Pn4	$(U_{11}+U_{12})/(U_{11}-U_{12})$ for Pn4	$\bar{d}$(Pn1−Pn4) (Å)[b]	Pn2−M−Pn2 angle (deg)[c]	ref
P	$Ca_{14}GaP_{11}$[d]	0.82	(9.2[e])	2.93	112.5	
As	$Ca_{14}GaAs_{11}$	0.0	12.5	2.96	113.0	4
	$Ca_{14}MnAs_{11}$	0.58		3.02	113.4	8
	$Eu_{13}NbAs_{11}$[d]	0.61	(10.9[e])	3.05	114.4	12
	$Sr_{14}GaAs_{11}$	0.70	(14.2[e])	3.11	114.7	5
	$Sr_{14}MnAs_{11}$	0.70		3.10	114.7	8
	$Sr_{13}NbAs_{11}$[d]	0.73	(25.9[e])	3.10	114.2	12
Sb	$Ca_{14}AlSb_{11}$[d]	0.0	1.8	3.20	114.0	2
	$Ca_{14}MnSb_{11}$	0.0	6.0	3.22	115.3	8
	$Ca_{14}ZnSb_{11.2}$	0.0	4.8	3.23	119.0	11
	$Eu_{14}MnSb_{11}$	0.0	1.9	3.26	118.6	9
	$Sr_{14}AlSb_{11}$	0.0	3.6	3.30	114.6	6
	$Sr_{14}MnSb_{11}$	0.0	3.4	3.31	115.9	8
	$Sr_{14}ZnSb_{11}$	0.37		3.34	119.0	11
	$Sr_{14}CdSb_{11.4}$	0.46		3.36	118.9	11
	$Ba_{14}AlSb_{11}$	0.0	7.4	3.37	117.9	6
	$Ba_{14}MnSb_{11}$	0.58		3.42	118.7	8
Bi	$Ca_{14}MnBi_{11}$	0.0	1.0	3.34	118.0	7
	$Sr_{14}MnBi_{11}$	0.0	1.8	3.42	118.7	7
	$Ba_{14}MnBi_{11}$	0.0	3.0	3.50	119.9	7

[a] For each Ae and Pn, ordered by M according to the *a* lattice dimension: Ga∼Al < Mn (∼Nb) < Zn < Cd. The Nb compounds lack one cation, while the Zn and Cd members usually contain extra Sb. Data for $Ca_{14}CdSb_{11.4}$ were omitted because of large differences in its lattice parameters and *c*/*a* ratio from the rest. [b] $\bar{d}$ = *d*(Pn1−Pn1)/2. [c] The larger of the Pn2−M−Pn2 angles is listed. [d] Refined at room temperature; all others are based on data collected at 130 K. [e] Result if refined unsplit.

average Pn4−Pn1 distance in the Pn_3^{7-} anion (=*d*(Pn1−Pn1)/2). The ordering in the table is virtually perfect. The magnitudes of the splittings of the Pn4 positions regularly increase with decreasing Pn size, increasing cation size, and, slightly, with increasing MPn_4 size for fixed Ae and Pn. In the same way, the average Pn−Pn distance for any Pn increases regularly when so ordered first by size of Ae and then M. A threshold for Pn4 splitting appears for each Pn. Furthermore, the need or opportunity to split the Pn4 position seems well described by the refined magnitudes of its ellipsoid asymmetry (column 4), suggesting that the Pn atom in $Ca_{14}GaAs_{11}$ and $Ba_{14}AlSb_{11}$ probably should have been split as well. The case for $Ca_{14}MnSb_{11}$ is less clear as U_{33} of Sb4 was larger than usual. (This argument is restricted by the significance that one can attach to thedisplacement ellipsoid values. The U_{iso} values for the unsplit Sb4 atom in the first six antimony phases listed range between 1.2 and 2.2 Å^2.)

The reason for the trends can be appreciated better through an examination of the cation polyhedron around the Pn_3^{7-} anions. This structural feature is shown for $Ca_{14}GaP_{11}$ in Figure 2 with the ellipsoids at the 99% probability level and with both 50% P4 sites drawn. The Ca−P separations marked by heavy lines range over 2.95−2.97 Å about P1 and 2.78 (Ca1)−3.00 Å (Ca2) about each of the split P4 positions. The calcium ions involved also have close interactions of 2.88Å and up with P2 (in GaP_4^{9-}) as well as with the isolated P3 (below), so the entire force field is not easily imagined. As far as the important Ca−Ca separations, which in the overall picture afford some definition of the tightness of the cation enclosure, double lines in Figure 2 mark the shorter distances, the wider members denoting the shorter 3.44 Å lengths and the narrower, 3.53−3.74 Å. Finally, the thin single lines represent still longer distances, from 3.82 Å (for Ca1−Ca2 within the antiprism faces and Ca4−Ca4) up to 4.11 Å (Ca2−Ca2). Some additional influences on this last group from other anions, P3 especially, will be noted later. For comparison, the Ca−Ca distance in CaO is 3.40 Å (×12), another classical matrix effect.

The size of the Ca−P interaction spheres about P1 and P4 (Pn1 and Pn4 in general) are very much determined by the intercation repulsions as well as Ca−P and Ca−Ca interactions elsewhere. With a centered (not disordered) P4 atom, the distorted square antiprism of neighboring cations would yield equal Ca1−P4 and Ca2−P4 distances of 2.964(2) (×4) and 3.202(3) (×4) Å, respectively, notably longer than the 2.88−3.05 Å separations for seven or eight cation neighbors about P2 (in GaP_4) and P3 (isolated) elsewhere in the structure. These overly large Ca−P4 separations about P4 must be considerably more important energetically than the pair of 2.93 Å P1−P4 bonds that would pertain, a long distance relative to ∼2.42 Å expected in the P_3^{7-} anion for half-bonds (2.20 Å for a single P−P bond).[19,20] The observed displacement of P4 from the poorly bonded central position in the cavity provides it with two Ca1 cations at 2.78 Å and two Ca2 ions at 3.00 Å as neighbors, half as many 0.20 Å closer, the longer Ca−P4 separations now being 3.19 and 3.44 Å, respectively. At the same time the P−P bonds, presumably a distinctly lesser factor energetically, go from two at 2.93 Å to one each at 2.52 Å, at least approaching a half bond, and 3.34 Å, or alternatively from P_3^{7-} to something toward P_2^{4-} and P^{3-}. The logarithmic nature of distance dependence on bond order that is usually approximated will always mean that an off-center displacement provides a gain in total bond order. The decrease in the magnitude of the Pn4 splitting in this family for larger Pn or, conversely, its increase with larger Ae, have common origins and provide virtually a continum in degrees of distortion, with P_3^{7-} the extreme. Thus the 13 independent Ca−Ca separations about P_3^{7-} marked in Figure 2 average 0.27 Å shorter than the respective ones around Sb_3^{7-} in $Ca_{14}AlSb_{11}$.[2] There seems to be no particularly good basis to attribute the general increase in overall Pn_3^{7-} dimensions (*d*(Pn1−Pn1) that is always observed with the larger and heavier cations (Table 5) only to an

(23) Goodman, A. W. *Analytic Geometry and the Calculus*; MacMillan Publishing Co.: New York, 1980; p 464−471.

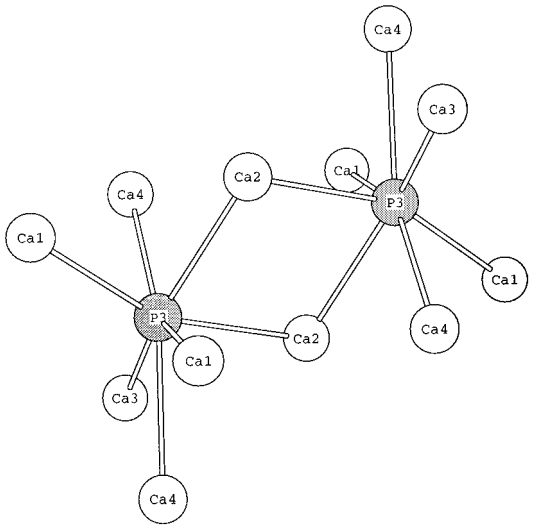

Figure 3. Environment of two isolated P^{3-} ions in $Ca_{14}GaP_{11}$ (~[1$\bar{2}\bar{3}$] view).

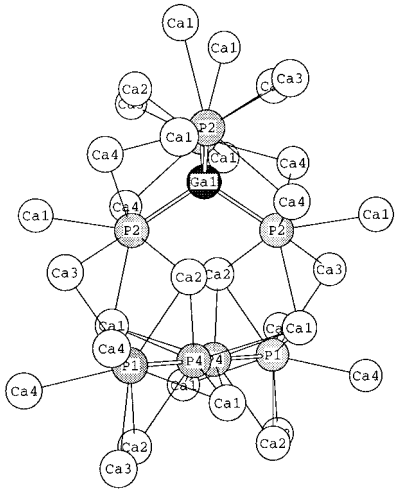

Figure 4. Perspective view showing the calcium ions (open spheres) about the P_7^{3-} and GaP_4^{9-} anions, especially those that are common and give them related distortions. (Compare Figures 1 and 2.) The 2-fold axis is vertical.

increased donor ability of the cation. Incidently, we are not aware of any evidence for the ordering of these displacements that would reduce the local symmetry at Pn_3^{7-} to C_2 or less.

There are also larger implications regarding phase stability as a function of the Ae and Pn sizes judging from the elemental combinations that have been reported (Table 5). We presume these reflect more about stabilities than a lack of trying. A phosphide phase is (so far) found only with the smallest Ca, but the arsenides form with Ca, Eu, Sr, the antimonides for all cations (Ca−Ba and Eu), and the bismuthides for Ca−Ba (and probably Eu). The implication of instability for phases combining the two smaller pnictide members with large Ae cations must extend beyond just the poor environment provided for the Pn_3^{7-} unit, perhaps illustrating excessive cation−cation repulsions about the small isolated Pn^{3-} anions as well. The coordination environment about the isolated P3 in the present case, Figure 3, is roughly a monocapped octahedron of calcium ions. The shorter Ca−Ca distances within this are 3.30 and 3.43 Å for Ca1−Ca4 and Ca3−Ca4, respectively (at the bottom of the Figure), 3.57 Å for Ca2−Ca4, and up. These cations are also common to the P_3^{7-} environment (Figure 2), some occurring with different P3 anions. The phosphide anions form a spiral chain parallel to the *c* axis. The closest contact between the isolated phosphide anions is 4.49 Å, far outside normal bonding distances.

The nominally tetrahedral anions $M(Pn2)_4^{9-}$ in this structure type have also been noted to show an increasing (but not always linear) angular distortion with increased cation size. As seen in Table 5, these angles increase uniformly within all $Ae_{14}MPn_{11}$ series with fixed M and Pn, with $Eu_{14}MnSb_{11}$ as the sole exception. (The Sr-(Zn,Cd)-Sb pair is a little off, but extra interstitial Sb is present in some of these as well.) This angular trend also correlates with the strong and presumably dominant interactions between the MPn_4^{9-} anion and the neighboring Ae^{2+} cations and the fact that the latter are in part common to the Pn_3^{7-} environment, where regular changes have already been recognized. As shown in Figure 4, a common (vertical) 2-fold axis along *c* bisects both the P_3^{7-} anions and the larger angle of the GaP_4^{9-} polyhedra. These Pn_3^{7-} units lie in [110] planes and equivalent directions in the structure, that is, at 45° to the faces of the cell at $z = {}^1/_8$, ${}^5/_8$, etc., such that a pair of Pn2 atoms in each tetrahedron lies across the Ca1−Ca2 edges at the top and bottom of Figure 2, each with close links to common Ca1, Ca2, Ca3 ions (plus Ca4 elsewhere). (The Ca4 in Figure 2 also bridge four Pn2 edges (with the smaller angles) on each tetrahedron, top of Figure 4.) The rational expansion of the cation polyhedron about the Pn_3^{7-} with Ae size already described thus appears to carry over to the included Pn2−M−Pn2 angle with fixed M. Of course, variations of the M−Pn2 bond lengths with M, and thence the Pn2−Pn2 "bite", means a series with M varying should also be regular, but not with both Ae and M changing at the same time.

This compound $Ca_{14}GaP_{11}$ represents the first phosphide example of this large family of structures. It contains the first example of the hypervalent P_3^{7-} anion,[24] albeit extremely distorted, in addition to the isolated GaP_4^{9-} anion. Further work on these compounds will be needed to assess the instability, or not, of other phosphide examples in this structure class. The small Yb^{2+} might be a useful variation.

Acknowledgment. The authors thank Professor S. Kauzlarich for providing a variety of thermal ellipsoid data, Dr. W. Hönle for information on the niobium derivatives, and Professor R. A. Jacobson and J. W. Anderegg for maintaining the single-crystal X-ray diffraction equipment and making it available to us.

Supporting Information Available: Extended table of data collection and refinement information (1 page); table of observed and calculated structure factors (6 pages). Ordering information is given on any current masthead page.

CM950396R

(24) von Schnering, H.-G. *Angew. Chem., Int. Ed. Engl.* **1981**, *20*, 33.